Biochemical and Biophysical Research Communications 390 (2009) 319–324

Contents lists available at ScienceDirect

Biochemical and Biophysical Research Communications

journal homepage: www.elsevier.com/locate/ybbrc

Erythromelalgia mutation L823R shifts activation and inactivation of threshold sodium channel Nav1.7 to hyperpolarized potentials

Angelika Lampert [a,b,c,1], Sulayman D. Dib-Hajj [a,b,c], Emmanuella M. Eastman [a,b,c], Lynda Tyrrell [a,b,c], Zhimiao Lin [d], Yong Yang [d], Stephen G. Waxman [a,b,c,*]

[a] Department of Neurology, Yale University School of Medicine, 333 Cedar Street, New Haven, CT 06510, USA
[b] Center for Neuroscience and Regeneration Research, Yale University School of Medicine, USA
[c] Rehabilitation Research Center, Veteran Affairs Connecticut Healthcare System, 950 Campbell Avenue, Building 34, West Haven, CT 06516, USA
[d] Department of Dermatology, Peking University First Hospital, Beijing 100034, China

ARTICLE INFO

Article history:
Received 12 September 2009
Available online 1 October 2009

Keywords:
Sodium channel
Pain
Mutation
Patch-clamp
Inactivation
Erythromelalgia

ABSTRACT

Erythromelalgia (also termed erythermalgia) is a neuropathic pain syndrome, characterized by severe burning pain combined with redness in the extremities, triggered by mild warmth. The inherited form of erythromelalgia (IEM) has recently been linked to mutations in voltage-gated sodium channel Nav1.7, which is expressed in peripheral nociceptors. Here, we used whole-cell voltage-clamp recordings in HEK293 cells to characterize the IEM mutation L823R, which introduces an additional positive charge into the S4 voltage sensor of domain II. The L823R mutation produces a ~15 mV hyperpolarizing shift in the midpoint of activation and also affects the activation slope factor. Closing of the channel from the open state (deactivation) is slowed, increasing the likelihood of the channel remaining in the open state. The L823R mutation induces a ~10 mV hyperpolarizing shift in fast-inactivation. L823R is the only naturally-occurring IEM mutation studied thus far to shift fast-inactivation to more negative potentials. We conclude that introduction of an additional charge into the S4 segment of domain II of Nav1.7 leads to a pronounced hyperpolarizing shift of activation, a change that is expected to increase nociceptor excitability despite the hyperpolarizing shift in fast-inactivation, which is unique among the IEM mutations.

Introduction

Voltage-gated sodium channel Nav1.7, which is expressed in peripheral nociceptors, has recently emerged as a major target in pain research. Loss-of-function mutations of Nav1.7 have been linked to complete insensitivity to pain [1–3]. Conversely, two severe inherited neuropathic pain syndromes, named erythromelalgia (also termed erythermalgia, IEM) and paroxysmal extreme pain disorder (PEPD) were linked to heterozygous mutations in Nav1.7 [4,5]. IEM is characterized by severe burning pain combined with redness in the affected extremities, triggered by mild warmth. While two cases have reported favorable therapeutic outcome using the sodium channel blockers carbamazepine [6], and mexiletine [7], severe pain can only be alleviated in most patients by extensive cooling of the affected body parts. All IEM mutations studied thus far result in a hyperpolarizing shift of activation, allowing the channel to open at more negative potentials compared to wild-type. The shift in Nav1.7 activation is a strong contributor to nociceptor hyperexcitability in IEM [8–11], with the apparent increase in excitability linked to the size of the hyperpolarization shift [12]. Fast-inactivation, on the other hand, is left unaltered for most or shifted to more depolarized potentials for some mutations [6,8,9,13]. This depolarizing shift in inactivation increases the fraction of available channels and may support hyperexcitability. Thus far, no naturally-occurring IEM mutation was reported to shift steady-state fast-inactivation to more hyperpolarized potentials.

Structurally, sodium channels are comprised of four domains (DI–DIV), each composed of six transmembrane segments (S1–S6), with S4 carrying a positively-charged residue at every third amino acid and segments S1–S4 act as the voltage sensor [14]. Depolarizing voltage steps lead to an outward movement of these

Abbreviations: Nav, voltage-gated sodium channel; IEM, inherited erythromelalgia; WT, wild-type Nav1.7; DI–DIV, domain I–IV; S1–S6, transmembranal segments 1–6.

* Corresponding author. Address: Rehabilitation Research Center Veteran Affairs Connecticut Healthcare System 950 Campbell Avenue, Building 34 West Haven, CT 06516, USA. Fax: +1 203 937 3801.
E-mail addresses: AngelikaLampert@web.de (A. Lampert), Sulayman.Dib-Hajj@yale.edu (S.D. Dib-Hajj), eeastma1@jhu.edu (E.M. Eastman), Lynda.Tyrrell@yale.edu (L. Tyrrell), ZhimiaoLin@bjmu.edu.cn (Z. Lin), DrYongYang@yahoo.com (Y. Yang), Stephen.Waxman@yale.edu (S.G. Waxman).
[1] Present address: Institute of Physiology and Pathophysiology, Friedrich-Alexander-University of Erlangen-Nuremberg, Universitaetsstr. 17, 91054 Erlangen, Germany.

0006-291X/$ - see front matter © 2009 Elsevier Inc. All rights reserved.
doi:10.1016/j.bbrc.2009.09.121

gating charges, followed by a conformational change inducing the transient opening of the channel pore and sodium ion flow within less than a millisecond. Mutations of S4 segments have been linked to inherited skeletal, cardiac and CNS sodium channelopathies [15–17], including IEM [18]. In this study, we used whole-cell patch-clamp recordings to investigate the effects on channel gating of the IEM mutation L823R [19], which introduces an additional positive charge into the DII/S4 (Fig. 1). The introduction of a sixth positively-charged residue to DII/S4 is predicted to make the channel more sensitive to voltage changes, so that the S4 should respond to a weaker depolarizing stimulus, compared to wild-type channels.

Materials and methods

Plasmids. The L823R mutation was introduced into hNav1.7$_R$ which carries a TTX-R version of human Nav1.7 cDNA [20] using QuickChange XL site-directed mutagenesis reagents (Stratagene, La Jolla, CA). Throughout the manuscript, WT refers to hNav1.7$_R$ and L823R to the mutated hNav1.7$_R$ channel construct. Human embryonic kidney cells (HEK293) were transfected with the mutant channel construct using Lipofectamine 2000 (In Vitrogen, Carlsbad, CA) according to the recommendations of the manufacturer. Transfected HEK293 cells, grown under standard culture conditions (5% CO_2, 37 °C) in Dulbecco's modified Eagle's medium supplemented with 10% fetal bovine serum, were treated with G418 for several weeks to derive a stable cell line that expresses the mutant channel.

Electrophysiology. Whole-cell voltage-clamp recordings [21] of HEK293 cells stably expressing the sodium channels Nav1.7$_R$, or L823R derivative were obtained with an EPC-9 amplifier (HEKA electronics, Lambrecht/Pfalz, Germany) using fire polished 1–1.5 MΩ electrodes (World Precision Instruments, Inc., Sarasota, FL, USA). The pipette solution contained (in mM): 140 CsF, 10 NaCl, 1 EGTA, and 10 HEPES; 302 mosmol (pH 7.4, adjusted with CsOH) and the extracellular bath contained (in mM): 140 NaCl, 3 KCl, 10 glucose, 10 HEPES, 1 $MgCl_2$, 1 $CaCl_2$, 0.0003 TTX; 310 mosmol (pH 7.4, adjusted with NaOH). All recordings were conducted at room temperature (~21 °C). The pipette potential was adjusted to zero before seal formation, and the voltages were not corrected for liquid junction potential. Capacity transients were canceled, and series resistance was compensated by 65–95%. Leakage current was subtracted digitally online using hyperpolarizing potentials applied after the test pulse (P/4 procedure). Currents were acquired using Pulse software (HEKA electronics, Lambrecht/Pfalz, Germany), filtered at 30 kHz for deactivation, and 2.9 kHz for all other protocols. The sampling rate was 100 kHz, except for inactivation protocols, for which it was set to 50 kHz. For current density measurements, peak currents were divided by the cell capacitance, as measured from the automated compensation by the Pulse software.

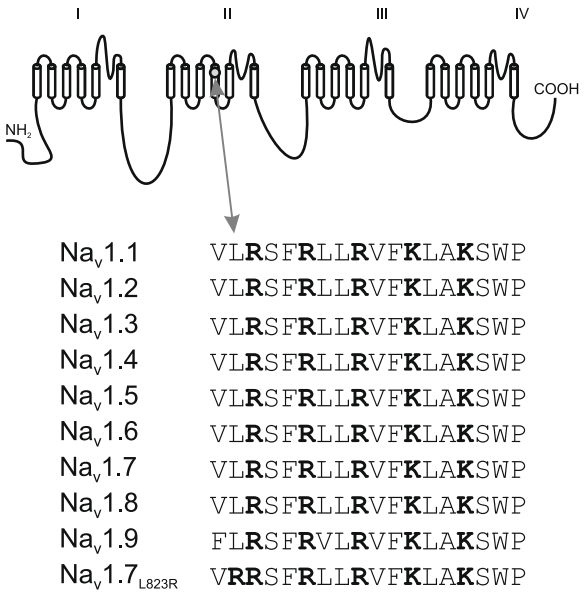

Fig. 1. Schematic of a voltage-gated sodium channel showing the location of the L823R mutation and the aligned sequences for the Nav1 DII/S4 linker. L823 residue is invariant in the nine members of the Nav1 family of voltage-gated sodium channels from humans.

Voltage protocols were carried out 4 min after establishing cell access. Standard current–voltage (*I–V*) families were obtained using 40 ms pulses from a holding potential of −120 mV to a range of potentials (−100 to +60 mV) in 5 mV steps with 5 s at - 120 mV between pulses. Peak values at each potential were plotted to form *I–V* curves. Activation curves were obtained by calculating the conductance *G* at each voltage *V*.

$$G = \frac{I}{V - V_{rev}}$$

with V_{rev} being the reversal potential, determined for each cell individually. Activation curves were fitted with the Boltzmann distribution equation:

$$G_{Na} = \frac{G_{Na,max}}{1 + e^{\frac{V_m - V_{1/2}}{k}}}$$

where G_{Na} is the voltage-dependent sodium conductance, $G_{Na,max}$ is the maximal sodium conductance, which was held at 1, $V_{1/2}$ is the potential at which activation is half-maximal, V_m is the membrane potential, and k is the slope factor.

Protocols for assessing steady-state fast-inactivation consisted of a series of prepulses (−130 mV to −10 mV) lasting 500 ms from the holding potential of −120 mV, followed by a 40 ms depolarization to −10 mV to assess the non-inactivated transient current. Individual pulse series were separated by 10 s. The normalized curves were fitted using a Boltzmann distribution equation:

$$\frac{I_{Na}}{I_{Na,max}} = \frac{1}{1 + e^{\frac{V_m - V_{1/2}}{k}}}$$

where $I_{Na,max}$ is the peak sodium current elicited after the most hyperpolarized prepulse, V_m is the preconditioning pulse potential, $V_{1/2}$ is the half-maximal sodium current, and k is the slope factor.

The rate of deactivation was measured using a short (0.5 ms) depolarizing pulse to −20 mV followed by a 50 ms repolarizing pulse to potentials ranging from −100 mV to −50 mV. Decaying current was then fitted with a single exponential function using PulseFit software (HEKA electronics).

Statistical analysis was carried out using SPSS software (SPSS Inc., Chicago, IL, USA) performing a Student's *t*-test. Results with $p < 0.05$ were considered significant. All data are presented as means ± SEM.

Results

Activation of L823R is shifted in a hyperpolarizing direction

We expressed wild-type and mutant Nav1.7 channels in HEK293 cells and used the whole-cell patch clamp method to assess the biophysical changes induced by the insertion of an additional positive charge into the voltage sensor by the IEM mutation L823R [19]. Both WT and L823R channels produce fast-gating sodium conductances (Fig. 2A) that opened and inactivated

within milliseconds when depolarizing potential steps were applied. Remarkably, L823R channels open at potentials as hyperpolarized as −55 mV whereas WT activates at voltages more depolarized than −40 mV (Fig. 2B). The conduction–voltage relation revealed a shift of the midpoint of activation (Boltzmann-Fit) of 14.6 mV, from −20.6 ± 1.8 mV for WT (n = 10) to −35.2 ± 1.4 mV for L823R (n = 14; Fig. 2B: $p < 0.001$ in a Student's t-test). Additionally, the L823R mutation renders the conduction–voltage relation less steep, with a slope factor of 11.5 ± 0.4 mV for L823R, and a slope factor of 8.3 ± 0.3 mV for WT ($p < 0.001$ in a Student's t-test).

Time-to-peak is slower for L823R compared to WT

Voltage-gated sodium channels open within milliseconds in a voltage-dependent manner. The more positive the applied test potentials, the faster the pore opens its permeation pathway. A measure for the speed of channel opening is the time from pulse onset until the current peaks (time-to-peak). Raw data shows that the introduction of an additional voltage into the voltage sensor of DII did not induce a faster opening rate of the channel pore (Fig. 3A), and in fact the L823R mutant channels appeared to open with slower kinetics at voltages between −5 mV and +35 mV (see inset Fig. 3A). This difference is especially significant, given that L823R channels open at much lower voltages. Correcting for this shift in activation reveals that the IEM mutant channels open more slowly over the entire voltage range investigated, and thus as a result of the shift in activation, the apparent time-to-peak does not differ more between WT and L823R when measured in whole-cell mode.

Deactivation is slower for L823R compared to WT

After opening of the channel's pore, closing can occur in two ways: deactivation, which refers to closing of the activation gate

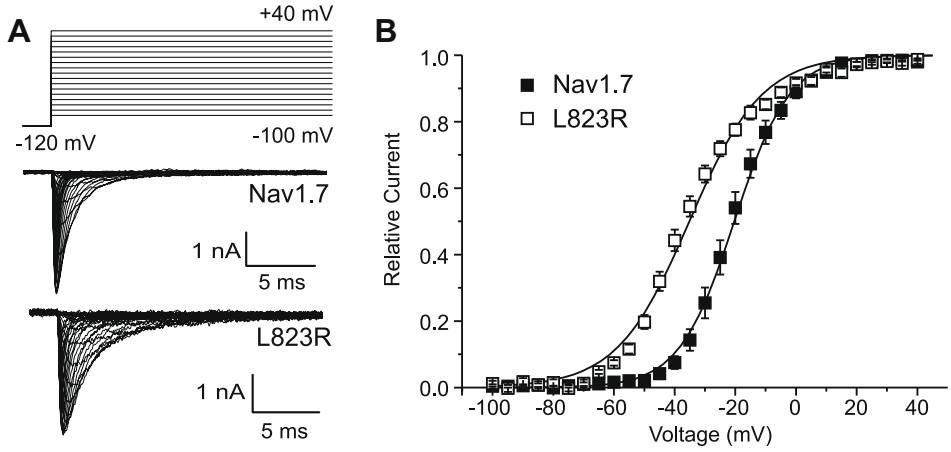

Fig. 2. Activation of L823R is shifted to more hyperpolarized potentials compared to WT. (A) Representative current traces evoked by step depolarizations from a holding potential of −120 mV to voltages varying from −100 mV to +40 mV (see protocol, top panel) in whole-cell patch clamp experiments on HEK293 cells stably expressing Nav1.7 (middle panel) or the IEM mutation L823R (lower panel). (B) Conductance–voltage relation showing a −14.6 mV shift to more hyperpolarized potentials of the activation midpoint for L823R (−35.2 mV ± 1.4 mV, n = 14, open squares) compared to WT (−20.6 ± 1.8 mV, n = 10, filled squares).

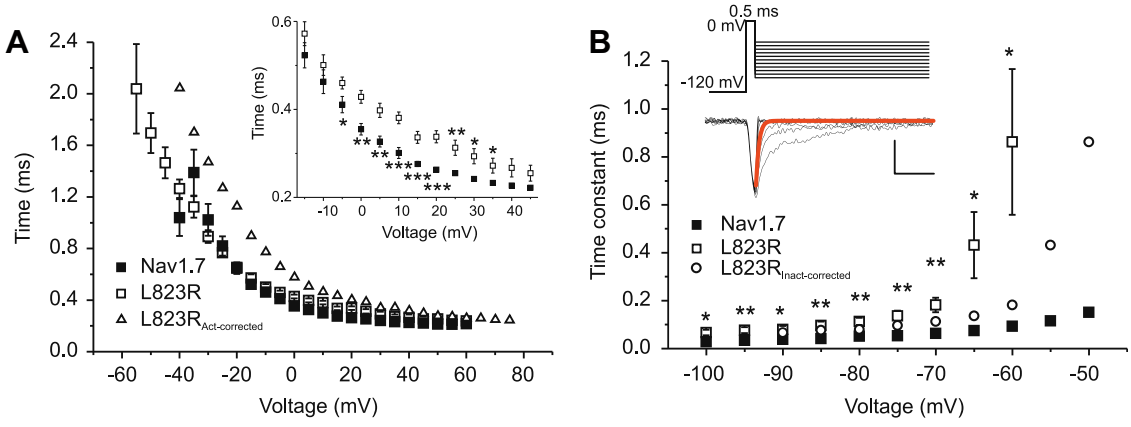

Fig. 3. Time-to-peak and deactivation is slower for L823R compared to WT. (A) Time-to-peak measured from pulse onset to maximal current at potentials between −55 mV (for L823R, open squares) or −40 mV (for WT, black circles) and +60 mV. L823R displays a large left shift in activation compared to WT (14.6 mV, see Fig. 2). Open triangles show values corrected for shift of activation of L823R. Inset: expanded graph showing significant differences in time-to-peak at voltages between −5 mV and +35 mV. $^{*}p < 0.05$, $^{**}p < 0.01$, $^{***}p < 0.001$ in a Student's t-test. (B) Time constants obtained from a single exponential fit to tail currents evoked by the protocol shown in the inset. L823R (open squares) deactivates slower at corresponding potentials compared to WT (filled squares). L823R displays a left shift in steady-state fast-inactivation at the potentials tested here compared to WT (9.8 mV, Fig. 4A). Correction for this shift reduces the difference in deactivation time constants between L823R and WT (open circles). $^{*}p < 0.05$, $^{**}p < 0.01$ in a Student's t-test. Inset: protocol used to assess deactivation. From a holding potential of −120 mV cells were stepped to −20 mV in order to activate channels. After 0.5 ms cells were re-polarized to potentials ranging from −100 mV to −30 mV for 50 ms, thereby evoking tail currents that result from deactivating channels, with little influence of fast-inactivation. Representative current trace of a cell expressing WT channels are shown. For clarity, traces in this figure were filtered digitally with 3 kHz and only every second trace is shown. Thick red line, example of a single exponential fit to tail current. Scale bars indicate 500 pA and 5 ms.

from the open state, and fast-inactivation, which occurs when the channel is inactivated by the block of the cytoplasmic opening of the pore by the binding of the inactivation particle to its receptor and blocking further sodium ion flow. In order to measure the time course of deactivation we used the protocol shown in Fig. 3B, inset. Channels are activated by a brief depolarization to 0 mV for 0.5 ms, and before a significant amount of fast-inactivation can occur, cells are re-polarized to potentials between −100 mV and −50 mV, evoking tail currents. A single exponential fit of the decaying current (red line in Fig. 3B inset) is used to measure the deactivation time constants (Fig. 3B), showing that they are slower for L823R at all potentials tested, possibly leading to a longer opening time of the channel during depolarizations.

Steady-state fast-inactivation of L823R is shifted to hyperpolarized potentials

In order to assess the voltage-dependence of steady-state fast-inactivation, we applied 500 ms prepulses to potentials ranging from −130 mV to −10 mV followed by a test pulse to −10 mV to determine the fraction of non-inactivated available channels (see protocol in Fig. 4A). Steady-state fast-inactivation is significantly shifted to more hyperpolarized potentials by 9.8 mV for L823R, compared to WT channels, with $V_{1/2}$ derived from Boltzmann fits of −76.9 ± 2.4 mV ($n = 9$) for WT and −86.7 ± 1.7 mV ($n = 14$; $p < 0.01$ in a Student's t-test) for L823R (Fig. 4A), whereas the slope factor remained unchanged (6.4 ± 0.2 for WT and 7.7 ± 0.7 for L823R). L823R is the first IEM mutation to display a left shift in steady-state fast-inactivation, which would, by itself, render neurons expressing these channels less excitable.

Current decay constants

The current decay occurring during a 40 ms test pulse is characteristic for the inactivation process of the channel protein. We performed a single exponential fit (as indicated in the inset in Fig. 4B) to current traces evoked at potentials between onset of activation and +40 mV. Interestingly, at lower potentials L823R inactivates more quickly than WT, while at more depolarized potentials it is slower, thereby producing more current than WT and at potentials between −25 mV and −10 mV no differences between WT and L823R decay time constant could be detected. On the other hand, if the data are corrected for the shift in activation that is relevant at the tested potentials (Fig. 4B, open triangles), and values at voltages at which a comparable amount of activation occurs are evaluated, L823R inactivates more slowly for the entire voltage range investigated.

Discussion

The positive amino acids in S4 of voltage-gated ion channels are thought to act as gating charges that move within the electrical field, inducing the conformational changes in the pore structure, thereby opening the channel's permeation pathway [22]. Introduction of an additional positive charge is expected to increase the gating currents and to facilitate the movement of the voltage sensor of that domain, resulting in an opening of the channel at lower potentials. We show in this study that the introduction of an additional positive charge into S4 of DII of Nav1.7 by the IEM mutation L823R leads to a pronounced hyperpolarized shift of activation. Previously, we have shown that an IEM mutation of a non-charged amino acid substitution in DI/S4, F214S [18], hyperpolarizes activation without altering voltage-dependence or kinetics of fast-inactivation [23]. In contrast, we show here that the L823R mutation shifts inactivation to more hyperpolarized potentials, which has not been previously described in IEM mutations, and thus retains the linkage between activation and inactivation of voltage-gated sodium channels.

Extensive studies of site-directed point mutations have been performed on voltage-gated sodium channels, and have revealed that not every charged amino acid has the same role in voltage sensing and that there are large differences between the S4 segments of the four domains. One-by-one substitutions of most charged residues in DI or DII by glutamine or glycine lead to a pronounced decrease in voltage-dependence [24–27]. Charge neutralizing substitutions in DIV, on the other hand, have smaller or no effects, and in DIII some mutations can even increase the channel's voltage sensitivity [26,28], stressing the different roles of the four domains during activation. The L823R in DII increases the voltage sensitivity of Nav1.7 (midpoint of activation is shifted by ~15 mV to more hyperpolarized potentials), which fits well with the results of charge neutralization in this particular domain.

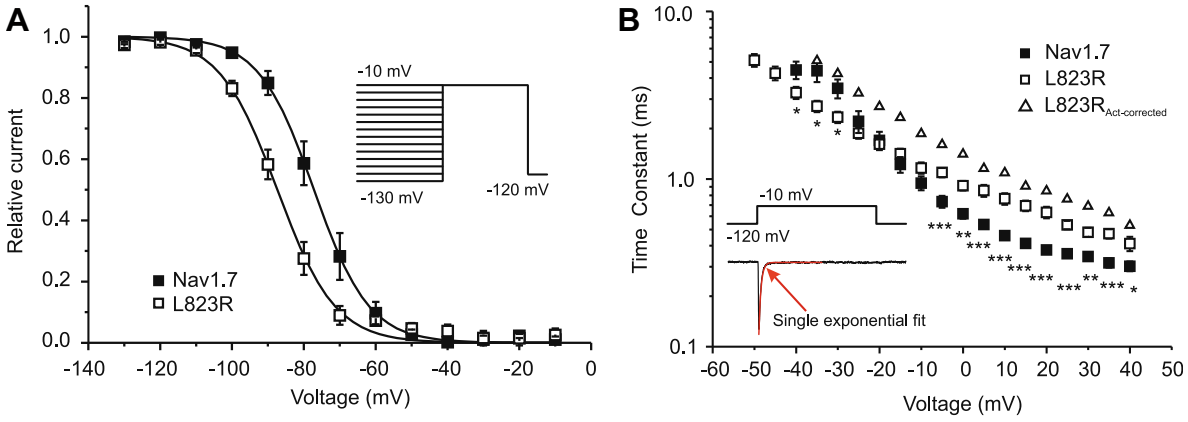

Fig. 4. Steady-state inactivation of L823R is shifted to more hyperpolarized potentials compared to WT. (A) Steady-state fast-inactivation of WT (filled squares, $n = 9$) and L823R mutant channels (open squares, $n = 14$). Available currents were assessed by a 40 ms pulse to −10 mV and plotted versus the applied prepulse potentials with increasing voltages starting from −130 mV (see inset for protocol). Cells were held at −120 mV for 10 s between pulses. Straight lines show Boltzmann fit of mean. (B) Inactivation decay time constants were obtained by fitting a single exponential function to current traces evoked by step depolarizations from a holding potential of −120 mV to the indicated voltages. Fits were performed from peak current to at least one third of test pulse duration (see inset, example trace at −10 mV). Filled squares, WT; open squares, L823R. L823R displays a large left shift in activation compared to WT (14.6 mV, Fig. 2). Correction for this shift unveils that L823R has slower inactivation kinetics than WT (open triangles). $^{*}p < 0.05$, $^{**}p < 0.01$, $^{***}p < 0.001$ in a Student's t-test.

In order to test for the effect of the IEM mutation on the kinetics of channel opening, we measured the time from pulse onset until the current peak (time-to-peak) and found that at potentials relevant during the late rising phase/peak of an action potential (between −5 mV and +35 mV), L823R opens slower than WT, whereas at the other potentials no significant difference was detected. When comparing voltages with similar channel activation, i.e. corrected for the shift of activation of L823R, this difference becomes even larger (Fig. 3A, open triangles). This is counterintuitive, as the conduction–voltage relation showed an increased voltage sensitivity for L823R and this could implement that the channel opens faster. Perhaps the extra charge in DII/S4, at a different phase of the amphiphatic α-helical structure of this segment relative to the other positively-charged residues, retards the movement of the DII/S4 segment of L823R mutant channel within the membrane plane.

Studies on the muscle sodium channel Nav1.4 with fluorescent labeling suggest that the voltage sensor of DIII moves at most hyperpolarized voltages, followed by DII and DI, whereas motion of DIV might not be necessary for channel activation [29]. Modeling studies support this order of movement also for Nav1.7 [30]. Introduction of an additional charge by the L823R substitution into DII, which moves at relatively hyperpolarized voltages, might be more effective than e.g. into DIV, which is predicted to move last. The additional gating charge might cause DII instead of DIII to move first. Because this unusual rearrangement within the channel protein might require more time for activation, pore opening might therefore take longer and, conservatively, time-to-peak would be expected to be consequently increased, as measured.

Deactivation kinetics revealed that L823R channels close slower than WT, thereby increasing the time of open channels at the potentials tested and most likely supporting hyperexcitability of nociceptors that express the mutant channel. Closing of the channel from the open state was measured after activating the channels with a brief pulse to 0 mV. At this potential, both WT and L823R channels should be activated to a comparable degree (Fig. 2B) and tail currents evoked after this short pulse should not be affected by changes in activation. Fast-inactivation on the other hand does occur to a different extent for WT and L823R at the potentials tested for tail currents (Fig. 4A). Correction of the effect of shifted fast-inactivation on deactivation time constants for L823R (Fig. 3B, open circles) reveals that the difference between WT and L823R is greatly reduced when comparing voltages at which a similar degree of channel inactivation occurs. The results suggest that the conformational changes that lead to closing of the channel pore are less severely affected by the L823R mutation, and that only the shift in fast-inactivation induced by the IEM mutation contributes to an apparent slower deactivation.

Most IEM mutations do not change fast-inactivation; some even shift its midpoint to more depolarized potentials, thereby increasing the window current and the excitability of an expressing cell [6,8,9,13]. Here we report for the first time a hyperpolarizing shift of steady-state fast-inactivation induced by an IEM mutation. The shift, by 9.8 mV, would reduce a window current and render the cells less excitable. The hyperpolarizing shift in activation might reflect coupling of activation and inactivation, with enhanced activation leading to an enhanced inactivation [31]. Interestingly, charge neutralizing mutations in DII of Nav1.4 induce a similar shift in steady-state fast-inactivation as we report here for the L823R mutation of Nav1.7 [25], suggesting a complex interplay between charges in S4 of DII and fast-inactivation. As L823R induces erythromelalgia in patients that are heterozygous for this mutation, we assume that the shift in activation to more hyperpolarized potentials by ∼15 mV is sufficient to overcome the predicted reduction in excitability induced by the ∼10 mV shift of steady-state fast-inactivation.

We have characterized the IEM mutation L823R, revealing a prominent shift of activation to more hyperpolarized potentials, slower time-to-peak and deactivation time constant and a left shift in steady-state fast-inactivation. Introduction of a positive charge into the voltage sensor of DII not only affects activation, but most probably also the rate of opening of the channel's pore and its inactivation, whereas the influence on closing of the pore seems rather small. We speculate that, in addition to rendering the voltage sensor more sensitive by introduction of an additional gating charge, the L823R mutation may induce wider conformational changes within the channel protein that might also affect movement of the S6 or other channel parts.

Acknowledgments

Support for research in S.G.W. laboratory comes from Medical Research Service and Rehabilitation Research Service, Department of Veterans Administration Rehabilitation Research and Development Service, and the Erythromelalgia Association. A.L. is supported by the Robert Bosch Foundation, Fast Track Program. Y.Y. is supported by Program for New Century Excellent Talents in University (NCET-06-0015) and Fok Ying Tong Educat ion Foundation (111039). The Center for Neuroscience and Regeneration Research is a Collaboration of the Paralyzed Veterans of America and the United Spinal Association with Yale University.

References

[1] Y. Goldberg, J. Macfarlane, M. Macdonald, et al., Clin. Genet. 71 (2007) 311–319.
[2] J.J. Cox, F. Reimann, A.K. Nicholas, et al., An SCN9A channelopathy causes congenital inability to experience pain, Nature 444 (2006) 894–898.
[3] S. Ahmad, L. Dahllund, A.B. Eriksson, et al., A stop codon mutation in SCN9A causes lack of pain sensation, Hum. Mol. Genet. 16 (2007) 2114–2121.
[4] S.D. Dib-Hajj, T.R. Cummins, J.A. Black, et al., From genes to pain: $Na_v1.7$ and human pain disorders, Trends Neurosci. 30 (2007) 555–563.
[5] J.P. Drenth, S.G. Waxman, Mutations in sodium-channel gene SCN9A cause a spectrum of human genetic pain disorders, J. Clin. Invest. 117 (2007) 3603–3609.
[6] T.Z. Fischer, E.S. Gilmore, M. Estacion, et al., Ann. Neurol. 65 (2009) 733–741.
[7] J.S. Choi, L. Zhang, S.D. Dib-Hajj, et al., Exp. Neurol. 216 (2009) 383–389.
[8] S.D. Dib-Hajj, A.M. Rush, T.R. Cummins, et al., Brain 128 (2005) 1847–1854.
[9] T.P. Harty, S.D. Dib-Hajj, L. Tyrrell, et al., J. Neurosci. 26 (2006) 12566–12575.
[10] A.M. Rush, S.D. Dib-Hajj, S. Liu, et al., A single sodium channel mutation produces hyper- or hypoexcitability in different types of neurons, Proc. Natl. Acad. Sci. USA 103 (2006) 8245–8250.
[11] P.L. Sheets, J.O. Jackson Ii, S.G. Waxman, et al., J. Physiol. (Lond.) 581 (2007) 1019–1031.
[12] C. Han, S.D. Dib-Hajj, Z. Lin, et al., Early- and late-onset inherited erythromelalgia: genotype-phenotype correlation, Brain 132 (2009) 1711–1722.
[13] C. Han, A.M. Rush, S.D. Dib-Hajj, et al., Ann. Neurol. 59 (2006) 553–558.
[14] W.A. Catterall, A.L. Goldin, S.G. Waxman, International union of pharmacology. XLVII. Nomenclature and structure–function relationships of voltage-gated sodium channels, Pharmacol. Rev. 57 (2005) 397–409.
[15] S.C. Cannon, Pathomechanisms in channelopathies of skeletal muscle and brain, Annu. Rev. Neurosci. 29 (2006) 387–415.
[16] A.L. George, Inherited disorders of voltage-gated sodium channels, J. Clin. Invest. 115 (2005) 1990–1999.
[17] C. Lossin, A catalog of SCN1A variants, Brain Dev. 31 (2009) 114–130.
[18] J.P. Drenth, R.H. Te Morsche, G. Guillet, et al., SCN9A mutations define primary erythermalgia as a neuropathic disorder of voltage gated sodium channels, J. Invest. Dermatol. 124 (2005) 1333–1338.
[19] K. Takahashi, M. Saitoh, H. Hoshino, et al., A case of primary erythermalgia, wintry hypothermia and encephalopathy, Neuropediatrics 38 (2007) 157–159.
[20] R.I. Herzog, T.R. Cummins, F. Ghassemi, et al., J. Physiol. (Lond.) 551 (2003) 741–750.
[21] O.P. Hamill, A. Marty, E. Neher, et al., Improved patch-clamp techniques for high-resolution current recording from cells and cell-free membrane patches, Pflugers Arch. 391 (1981) 85–100.
[22] F.H. Yu, W.A. Catterall, Overview of the voltage-gated sodium channel family, Genome Biol. 4 (2003) 207.
[23] J.S. Choi, S.D. Dib-Hajj, S.G. Waxman, Inherited erythermalgia. Limb pain from an S4 charge-neutral Na channelopathy, Neurology 67 (2006) 1563–1567.

[24] W. Stuhmer, F. Conti, H. Suzuki, et al., Structural parts involved in activation and inactivation of the sodium channel, Nature 339 (1989) 597–603.
[25] K.J. Kontis, A.L. Goldin, Sodium channel inactivation is altered by substitution of voltage sensor positive charges, J. Gen. Physiol. 110 (1997) 403–413.
[26] L.Q. Chen, V. Santarelli, R. Horn, et al., A unique role for the S4 segment of domain 4 in the inactivation of sodium channels, J. Gen. Physiol. 108 (1996) 549–556.
[27] S. Sokolov, T. Scheuer, W.A. Catterall, Gating pore current in an inherited ion channelopathy, Nature 446 (2007) 76–78.
[28] K.J. Kontis, A. Rounaghi, A.L. Goldin, Sodium channel activation gating is affected by substitutions of voltage sensor positive charges in all four domains, J. Gen. Physiol. 110 (1997) 391–401.
[29] B. Chanda, F. Bezanilla, Tracking voltage-dependent conformational changes in skeletal muscle sodium channel during activation, J. Gen. Physiol. 120 (2002) 629–645.
[30] A. Lampert, A.O. O'Reilly, S.D. Dib-Hajj, et al., J. Biol. Chem. 283 (2008) 24118–24127.
[31] C.M. Armstrong, Sodium channels and gating currents, Physiol. Rev. 61 (1981) 644–683.